

## **Detection and Quantification of Lead in Drinking Water via Flame Atomic Absorption Spectroscopy (FAAS), Inductively Coupled Plasma Quadrupole Mass Spectrometry (ICP-Q-MS), and Microfluidic Paper-Based Analytical Devices ( $\mu$ PADs)**

### **Abstract**

Contamination of drinking water with heavy metals, especially lead, is detrimental to the health of the consumers at high enough concentrations. It is necessary to find an inexpensive, simple, and accurate method of detecting heavy metals at such low concentrations. FAAS, ICP-Q-MS, and  $\mu$ PADs were all used in attempt to achieve this goal.

In the FAAS portion of this experiment, various aqueous lead standards were made to be calibrants for the construction of a calibration curve. The samples with unknown concentrations of lead were tested using FAAS and then quantified using the calibration curve. For the purpose of data analysis, linear regression statistics, t-Tests, and f-Tests were utilized. Using the class data set, the LOD and LOQ of the spectrophotometer were found to be 0.0291 and 0.0970, respectively. The concentrations of lead in samples A, B, C, A Duplicate, LFM, and LFB were found to be 1.6, 2.56, 3.19, 1.68, 1.14, and 1.50 ppm, respectively. All of the samples were able to be quantified. FAAS is a reliable method of quantification of lead in water, as long as the samples are within the parameters of the instrument.

In the ICP-Q-MS portion of this experiment, lead and iron in water from the Ohio State University Columbus Campus was quantified and determined to be well below the EPA recommended maximum Pb concentration of 15 ppb and Fe concentration of 300 ppb.<sup>(EPA)</sup> Various standards were made by Group 1 and by the TERL (Trace Element Research Laboratory) to act as calibrants for the construction of a calibration curve for ICP-Q-MS (Inductively Coupled Plasma Mass Spectrometry). Using the TERL calibration curve for quantification, five water fountain samples and their blanks were tested for lead and iron using ICP-Q-MS. For the purpose of data analysis, the average and standard deviation of the concentration of each sample and linear regression statistics were utilized. After background subtraction and drift correction, the limit of detection and limit of quantification of the ICP-Q-MS instrument were found to be  $-9.94\text{e-}8$  and  $-3.31\text{e-}7$ , respectively. ICP-Q-MS is a reliable method of quantification of lead and iron in drinking water, as long as the samples are within the parameters of the instrument and the calibration curve is accurate. The lead and iron concentrations in each sample were found to be within the EPA limits.

In the  $\mu$ PAD portion of this experiment, a  $\mu$ PAD was developed for the purpose of detecting lead in drinking water.  $\mu$ PADs are cheap and portable, making them ideal for in-home or field water testing. The  $\mu$ PAD involves a dual-well design: one reaction well and one control well. Depending on the colors of the wells after application, the user is able to tell if their water has a concentration of lead above or below the threshold concentration, 20 ppm. The design also requires a preconcentration step and an accumulation step in order to increase the effective molar equivalent of lead and therefore have a LOD of 20 ppm.

ICP-Q-MS can detect the lowest concentrations, followed by FAAS and then  $\mu$ PADs.  $\mu$ PADs cannot currently detect lead concentrations as low as the maximum legal concentration, 15 ppb. Therefore,  $\mu$ PADs can't yet be used practically for this purpose, but in the future, they may be able to test for lead in drinking water cheaply and easily.

## Introduction

Quantification of lead in drinking water is an important analytical procedure that can impact the health of people both regionally and globally. Water treatment plants all around the world must accurately determine the amount of lead in their water in order to ensure it is in accordance with health regulations. If this analysis fails to be accurate, the community reliant on that water supply is susceptible to lead poisoning, reproductive problems, nervous system damage, and more.<sup>1</sup> Unfortunately, drinking water has become the primary source of exposure to lead in the United States.<sup>1</sup> One of the worst examples of water contamination is Flint, Michigan. The city opened their own water treatment plant in 2014 in an attempt to lower the price. Unfortunately, this was done so improperly, and the water was being drawn from a polluted river. This deadly combination caused extreme contamination in the city's drinking water. To this day, Flint still does not have a water supply that is suitable for humans to drink or bathe in.<sup>2</sup> The Environmental Protection Agency's Lead and Copper Rule of 1991 has conducted research to determine the maximum safe concentration of lead in drinking water to be 15 ppb.<sup>2</sup> Some Flint homes were found to have an astonishing 68 ppb lead in their water.<sup>2</sup> Treatment facilities should consistently hold their water quality to at least that high of a standard. In addition to lead, iron is another heavy metal that can enter the body through drinking water and cause detrimental effects in high enough concentrations. Most cases of iron poisoning occur due to iron supplement overdose, especially in the case of children consuming adult vitamins.<sup>3</sup> A toxic level of iron is 20 mg/kg, causing metabolic acidosis and organ failure.<sup>3</sup> Therefore, the EPA sanctioned maximum legal concentration of iron in drinking water is 300 ppb.<sup>4</sup>

Flame Atomic Absorbance Spectroscopy (FAAS) is a method of quantifying an unknown concentration of lead in water that will be explored in this paper. FAAS measures concentrations based on absorption of light, so it has the ability to distinguish one element from another in a complex mixture. In the first step of FAAS, sample solution is drawn into the pneumatic nebulizer by rapid airflow past the tip of the sample capillary. As the liquid leaves the capillary, it breaks into a fine mist which hits a glass bead, breaking the mist into smaller particles to form an aerosol.

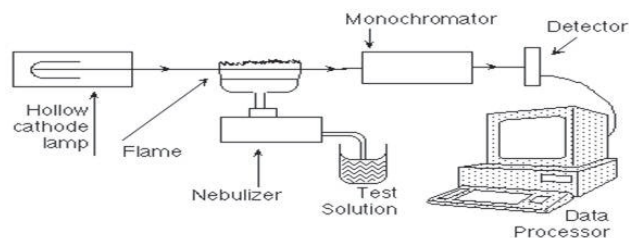


**Figure 1:** Diagram of a Flame Atomic Absorption Spectrometer<sup>5</sup>

In the premix burner, the aerosol, air, and fuel mix together and large droplets are removed by baffles. The aerosol then exits the premix burner and enters the flame, containing only about 5% of the initial sample. The liquid evaporates, and the remaining solid is atomized. A hollow cathode lamp containing vapor of the same element being analyzed is directed through the sample in the flame. The wavelengths of light are 217 and 283.3 nm. The intensity of the transmitted radiation is measured by a photon transducer. Each metal has its own unique wavelength of absorbance, allowing for the determination of what metals are in the sample.<sup>6</sup> This mechanism is displayed in Figure 1. Additionally, the intensity of the absorption gives information about the concentrations of said metals. The determination of concentration, however, is limited to a certain range. The instrument cannot detect extremely low concentrations, and it will not give accurate measurements for extremely high concentrations. Other limitations of this instrument include noise levels (shot, Johnson, white) and interference (background and chemical). The instrument takes measurements

of each sample three times, and software provides the average and standard deviation of the three. Other than water, FAAS is commonly used to analyze soil, sediment, and biota samples.<sup>7</sup>

ICP-Q-MS is a method of quantifying an unknown concentration of lead and iron in water that will be explored in this paper. It is an important method of analysis because it can measure very low concentrations of metals, down to the part per trillion. Therefore, ICP-Q-MS can give accurate readings of the relatively low concentrations of metals in drinking water. Within the instrument, liquid samples were introduced into a quartz concentric nebulizer and flowed into a quartz cyclonic

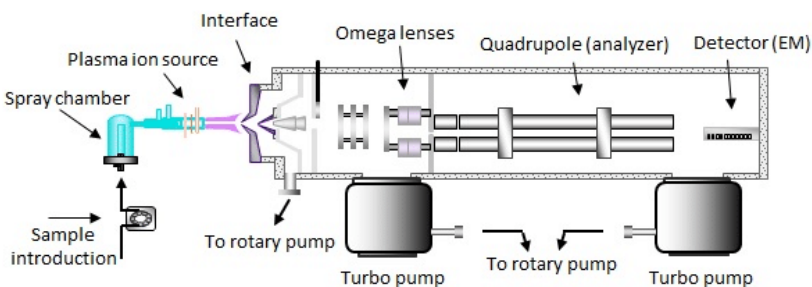


**Figure 2:** Schematic of an ICP-Q-MS instrument<sup>9</sup>

spray chamber, converting the sample to its plasma state.<sup>8</sup> The plasma state of a sample is comprised of its substituent atoms and ions. The flow rate is controlled by the peristaltic pump. From there, the beam of atomized sample is refined by multiple cones to reduce scatter before it reaches the quadrupole mass separator, which selects for atoms of a certain mass. Next, the ions of the desired mass continue into a detector that counts the number of ions of each mass that are deposited.<sup>10</sup> Each metal has its own unique atomic mass, allowing for the determination of which individual metals are in the sample.<sup>10</sup> Challenges arise when there are multiple ions in the sample that have the same mass, isobaric ions, because it becomes difficult to differentiate between the two. In order to circumnavigate this problem, reactions can be performed with an inert gas such as He or NH<sub>3</sub>, or high-resolution mass spectrometry can be utilized. This schematic of this instrument is displayed in Figure 2. The intensity of the volume of each metal atom detected gives information about the concentrations of said metals. The determination of concentration, however, is limited to a certain range. The instrument cannot detect extremely low concentrations, and it will not give accurate measurements for extremely high concentrations. Additionally, a method blank was tested and subtracted from all sample readings to ensure that background noise is cancelled. This background noise could possibly be caused by atmospheric lead in the TERL. The instrument takes measurements of each sample three times, and software provides the average and standard deviation of the three. Other than detecting heavy metals in drinking water, ICP-Q-MS is commonly used to detect trace elements in ground water and sediment samples.<sup>9</sup>

The first  $\mu$ PAD was developed in 2007 by Martinez et al. to fill the need for an inexpensive, low volume, portable point-of-care bioassay.<sup>11</sup> Lateral flow assays were the instruments  $\mu$ PADs had been developed to compete with. Lateral flow assays can only test one analyte at a time, they are qualitative, and they are very complex. On the other hand, the  $\mu$ PAD was developed to detect multiple analytes, be qualitative or quantitative, require a smaller sample volume, and be more simple to produce than lateral flow assays.<sup>13</sup>  $\mu$ PADs and paper substrates are desirable due to the aforementioned properties and the fact that they are renewable, light, portable, and easy to use and interpret. In general,  $\mu$ PADs consist of a hydrophilic paper substrate with hydrophobic boundaries to contain the sample. Capillary forces disperse the sample across the exposed paper area, where it can reach any reagents or reactants that have been placed on the  $\mu$ PAD. Some current applications of  $\mu$ PADs include neurotransmitter detection, cancer diagnosis and treatment, cell and tissue culture growth and amplification, drug discovery and determination, detection and

identification of microorganisms.<sup>13</sup> When a chemical indicator is used in conjunction with a  $\mu$ PAD, the  $\mu$ PAD has the ability to detect the analytes that react with the indicator. This method of detection is comparable to an ion selective electrode because they both are very accurate and selective methods of detecting a certain analyte in specific. Preconcentration steps are often used with  $\mu$ PADs in order to decrease the LOD by effectively increasing the molar equivalent of the analyte without increasing the overall concentration of the analyte. In the case of lead, a 3% sodium carboxymethylcellulose in water mixture with zirconium silicate is used. The zirconium silicate is adsorbent, meaning that it binds to lead and forms complexes that allow for the aforementioned results.<sup>14</sup>

$\mu$ PADs seem to be a viable option for field and in-home testing for heavy metals in water samples. Many of the locations in the world with the worst water contamination issues, such as Flint, are poorer areas. Most of the civilians are not able to afford the expenses of sending water samples to a lab for testing. Therefore, they need a cheap, accurate, and easy method of testing their water for dangerous contaminants.  $\mu$ PADs may be the answer to that problem due to all of their advantageous characteristics. Some  $\mu$ PADs are even able to detect multiple analytes at once, meaning that users may be able to detect for multiple heavy metals at once. Developing  $\mu$ PADs for the purpose of detecting lead in drinking water would allow citizens to test their own water for a low price.

## Methods

There were three samples in the FAAS portion of experiment, each containing an unknown concentration of lead in tap water from the lab. The chemicals used in this experiment were nano-pure water from McPherson Laboratory, lead stock solution (1000 ( $\pm$  10) ppm Pb in 3% HNO<sub>3</sub> by volume) from Sigma Aldrich in Milwaukee, IL, and LC Grade 70% HNO<sub>3</sub> solution from Sigma Aldrich in Milwaukee, IL. The materials used in this experiment include nine 50 ( $\pm$  0.05) mL Fisher Scientific volumetric flasks, one 100 ( $\pm$  0.08) mL Fisher Scientific volumetric flask, one 250 ( $\pm$  0.2) mL Fisher Scientific volumetric flask, Fisher Scientific Pasteur pipettes, two Fisher Scientific micropipettes (one 100 ( $\pm$  1)  $\mu$ L and one 1000 ( $\pm$  0.8)  $\mu$ L), and seven Fisher Scientific test tubes. The micropipettes could not accurately deliver less than 10  $\mu$ L of fluid. The instrumentation used for FAAS was a Shimadzu AA-7000. For this instrument, the limit of detection was calculated to be 0.0291 ppm, and the limit of quantification was calculated to be 0.0970 ppm using Equations (4) and (5) and the Class Data. All dilutions and measurements were conducted at standard conditions for temperature and pressure.

Samples A, B, and C were obtained from the TA and acid preserved with the addition of 1 mL HNO<sub>3</sub> to 49 mL of each sample in 50 ( $\pm$  0.05) mL volumetric flasks. This preservation made each sample 2% HNO<sub>3</sub> by volume. Then, fifteen calibrants of varying concentrations were prepared through volumetric dilutions of the lead stock solution (calculations in Excel). Seven of these calibrants were prepared by Group 1 (0.0, 0.050, 0.50, 1.0, 2.0, 5.0, and 7.0 ppm), while the remaining calibrants were prepared by the rest of the class (0.10, 0.20, 0.30, 0.40, 10, 12, 15, and 20 ppm). These calibrants were made by putting a small amount nano-pure water in a volumetric flask, adding a calculated amount of lead stock solution to reach the desired concentration, and adding 1 mL HNO<sub>3</sub> for preservation. The flasks were then capped and inverted twenty times. Then, the volumetric flask was filled to the point at which the bottom of the meniscus is touching the marked line. The flasks were again capped and inverted twenty times. A 50 ( $\pm$  0.05) mL volumetric flask was used for each concentration of calibrant, except 0.050 ppm. Because of the small concentration, a 250 ( $\pm$  0.2) mL flask was utilized for 0.050 ppm.



Next, a Lab Fortified Blank (LFB) and a Lab Fortified Matrix (LFM) were prepared using nearly the same method. To prepare the LFM, two dilutions were done. A known amount of lead stock solution (0.125 mL) was added to a duplicate of unknown sample B in a 50 ( $\pm$  0.05) mL volumetric flask to approximately double the concentration. Next, the resulting solution was diluted by half in a 100 ( $\pm$  0.08) mL volumetric flask to form the LFM. Finally, the LFB was prepared by adding an arbitrary amount of lead stock solution to the method blank (the concentration of zero calibrant). Group 1 chose to make the LFB 3 ppm. Both the LFB and LFM were acid preserved to be 2% HNO<sub>3</sub> by volume.

Once each sample, calibrant, LFM, and LFB was complete, they were each poured into individual test tubes. The test tubes were loaded into the Shimadzu AA-7000 to be analyzed by FAAS. The instrument collected data as previously explained, and the computer software gave the final output. The data from this particular experiment will be referred to as the Group Data. The following week, the entire class collectively made one set of samples following the same procedure. This will be referred to as the Class Data.

For the ICP-Q-MS portion of this experiment, a total of ten samples were analyzed. Drinking water samples from water fountains at each of these locations were obtained: Barrett House, Busch House, the RPAC, Campbell Hall, and Hopkins Hall. 1000 mL wide mouth polyurethane sample collection bottles were used as the vessels. All ten samples were collected between 8:29 and 8:47 AM on the morning of February 13<sup>th</sup>, 2019. The weather during sampling was 26 degrees Fahrenheit, windy, and cloudy. The air quality index was 26.

Additionally, a NIST (National Institute of Standards and Technology) sample of Lake Michigan water with known metal concentrations was tested. The standards prepared by Group 1 included nine solutions of nanopure water containing the following concentrations of each of the tested metals: 10 ppt, 50 ppt, 100 ppt, 300 ppt, 500 ppt, 700 ppt, 1 ppb, 3 ppb, 5 ppb. In order to produce these samples, heavy metal stock solutions of 1000 ( $\pm$  10) ppm ICP-MS grade lead and iron in 3% HNO<sub>3</sub> by volume were used. Both of these heavy metal stock solutions were from Sigma Aldrich in Milwaukee, IL. The TERL also prepared a separate set of standards. The first contained 0.05 ppb Pb and 5 ppb Fe. The second contained 0.10 ppb Pb and 10 ppb Fe. The third contained 0.25 ppb Pb and 25 ppb Fe. The fourth contained 0.50 ppb Pb and 50 ppb Fe.

The materials used in this experiment include nine 50 ( $\pm$  0.05) mL Fisher Scientific volumetric flasks, Fisher Scientific Pasteur pipettes, and a 100 ( $\pm$  1)  $\mu$ L Fisher Scientific micropipette. The instrumentation used in this experiment included a Fischer Scientific Accumet AB150 pH/mV meter and the ICP-Q-MS instrument, the PE SCIEX Elan 6000. For the PE SCIEX Elan 6000, the limit of detection (LOD) was calculated to be  $-9.94\text{e-}8$  using TERL standards with Pb,  $-9.16\text{e-}5$  using TERL standards with Fe,  $-7.02\text{e-}8$  using Group standards with Pb, and  $-3.02\text{e-}5$  using Group standards with Fe. The limit of quantification (LOQ) was calculated to be  $-3.31\text{e-}7$  using TERL standards with Pb,  $-3.05\text{e-}4$  using TERL standards with Fe,  $-2.34\text{e-}7$  using Group standards with Pb, and  $-1.01\text{e-}4$  using Group standards with Fe. The LOD was calculated with Equation (4) and the LOQ was calculated using Equation (5). The accepted LOD and LOQ will be the values found using the TERL standards with Pb. All dilutions and measurements were conducted at standard conditions for temperature and pressure.

While sampling, a plastic field blank bottle filled with nanopure water from the McPherson Lab was left open to take in any heavy metal contaminants from the air that may have gotten in the real sample. While filling the sample bottle, the first drops of the water out of the fountain were purposely caught. Once all sample bottles were filled and returned to McPherson, they were each

acid preserved to be below a pH value of 2 using LC Grade 70%  $\text{HNO}_3$  solution from Sigma Aldrich in Milwaukee, IL. The samples were then stored in a refrigerator. In order to make the Group-produced standards, serial dilutions were done using the heavy metal stock solutions and the McPherson nanopure water to yield the nine concentrations of stock solution. This process was done volumetrically, using 50 ( $\pm 0.05$ ) mL volumetric flasks and a micropipetter to transfer small amounts of the liquid that needed to be diluted. Finally, the samples and standards were transported to the TERL where the PE SCIEX Elan 6000 is housed. The instrument was first calibrated with both sets of standards and then each sample and blank were tested individually by placing the aspirator in the sample bottle and letting the instrument run. A method blank was tested at the beginning of the day and at the end to account for possible drift.

In order to analyze this data, four calibration curves were made: one with the Group's standards and one with the TERL's standards. Linear squares analysis was employed to create the calibration curves for analysis of the samples.

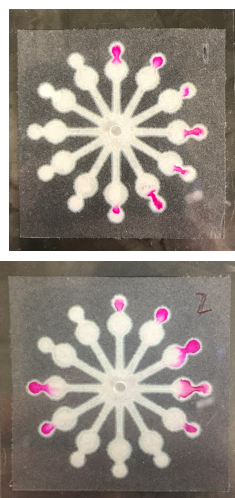


**Figure 3:** HCl with 0.095 M NaOH  $\mu$ PAD  
Top: accurate run  
Bottom: inaccurate run

For the  $\mu$ PAD portion of this experiment, preliminary tests were done using paper acid/base titrations. The purpose of this test was to develop an understanding of the intricacies of  $\mu$ PADs. 12-well snowflake design  $\mu$ PADs were provided along with 0.095 and 0.0944 M NaOH, 1.014 M HCl, solid KHP, and 0.25% (w/v) PHTH in ethanol. From these, 0.0238, 0.0475, 0.0950, 0.190, and 0.380 M HCl standards were made. Additionally, KHP standards were made at the same concentrations. The calculations can be found in Excel. After the  $\mu$ PADs were cut out, the wax was melted, and taped, 0.3  $\mu$ L PHTH was placed in each detection well (the outer wells). Then, 1.0  $\mu$ L of HCL or KHP was added to each of the reaction wells. Finally, the  $\mu$ PAD was placed in the plastic holder and 53  $\mu$ L of NaOH was added to the center well slowly. Since HCL and KHP react with PHTH in a 1:1 molar ratio, the wells that are pink have acid of an equivalent or lower molarity than the NaOH. Inversely, the wells that stay white have acid of a greater molarity than the NaOH. The concentrations of acid were applied to the  $\mu$ PAD in the order of increasing concentration clockwise starting from the top, with two wells of each

concentration.  $\mu$ PADs were run with all of the possible combinations of reagents: HCl with 0.095 M NaOH, HCl with 0.0944 M NaOH, KHP with 0.095 M NaOH, and KHP with 0.0944 M NaOH. Good results were obtained for each combination; for example, Figure 3 displays the  $\mu$ PAD with HCL and 0.095 M NaOH. The pink color stops at the point at which the molarity of the acid exceeds the molarity of the base.

Many lessons about  $\mu$ PADs were learned during these preliminary tests. First, it was determined that taping the back of the  $\mu$ PAD is necessary to stop the sample from just wicking straight through onto the table. It was also noted that the longer a  $\mu$ PAD is left on the hot plate, the more the wax melts, and there narrower the lanes get. The  $\mu$ PAD should be heated enough for all of the wax to melt through, but not long enough for the lanes to get considerably narrower. If the lanes become too narrow, wicking ability is impaired. Additionally, it was determined that  $\mu$ PADs may not be 100% reproducible. The same exact test done two times in a row yielded slightly different results for unknown reasons, as displayed in Figure 3. It is possible that the incorrect acid concentration was added to the problem wells. Finally, it was noted that  $\mu$ PADs

cannot be quantitative devices because there are too many confounding factors such as the acidity of the paper reacting with the indicator and the NaOH travelling to different wells at different speeds.

When the lead detection development process began, thirteen different concentrations of lead standards were tested throughout the development process. These standards included 0, 3, 6, 9, 12, 15, 30, and 100 ppb and 1, 10, 20, 40, 80, and 100 ppm. They were all made through the volumetric dilution of lead stock solution (1000 ( $\pm 10$ ) ppm Pb in 3% HNO<sub>3</sub> by volume) from Sigma Aldrich in Milwaukee, IL with nano-pure water from McPherson Laboratory. The dilution calculations can be found in Excel. The other chemicals used include sodium rhodizonate solid, carboxymethylcellulose solid, and zirconium silicate, all from Sigma Aldrich in Milwaukee, IL. Additional materials used include Whatman 1 filter paper, packing tape, scissors, seven 50 ( $\pm 0.05$ ) mL Fisher Scientific volumetric flasks, Fisher Scientific Pasteur pipettes, a 10 ( $\pm 0.2$ )  $\mu$ L Fisher Scientific micropipette, a Fischer Scientific hot plate, and a wax printer. The instrumentation used in this experiment includes a Fischer Scientific analytical balance, the  $\mu$ PADs themselves, and the human eye.

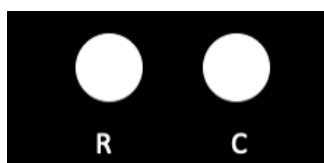


**Figure 4:** (C) well doesn't turn orange

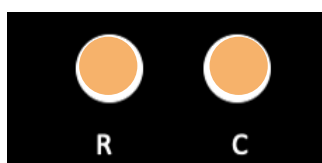


**Figure 5:** Both wells turn orange

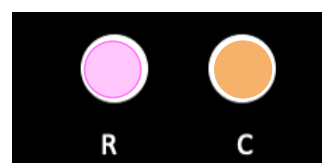


**Figure 6:** (R) well turns pink and (C) well stays orange

In order to produce a functional  $\mu$ PAD with a LOD of 20 ppm and aliquot size of 3  $\mu$ L, the  $\mu$ PAD design must first be printed on Whatman 1 filter paper using a wax printer. The design is then cut out with scissors and placed on a hot plate wax-side-up until the wax melts through the paper. Once this occurs, the back of the  $\mu$ PAD is taped with packing tape. The  $\mu$ PAD is then coated in the preconcentrate solution with a medicine dropper and a gloved finger. The excess is wiped off and the preconcentrate is allowed to dry. One dry, the  $\mu$ PAD is ready for use. The user drops 6 aliquots of sample water onto the reaction well and lets it dry completely. The user then drops 1 aliquot of 0.05% sodium rhodizonate indicator onto each well and observes the changes. If the Control (C) well does not turn orange (Figure 4), either the  $\mu$ PAD or the indicator is defective, and the test is inconclusive. If both wells turn orange (Figure 5), less than 20 ppm lead is in the sample. If the Reaction (R) well turns pink and the Control (C) well stays orange (Figure 6), 20 ppm or more lead is in the sample. If this is the case, it is advised that the user seek further testing due to the extreme toxicity of their water.

Ample safety measures were taken throughout these experiments. Proper personal protective equipment was worn by all of Group 1, including nitrile gloves, a lab coat, and goggles. Additionally, the 70% HNO<sub>3</sub> solution was kept in the fume hood. Group 1 took precautions in order to ensure accuracy and precision in this procedure. The same group member carried out the same part of the procedure every time to limit variability.

## Equations

(1) $s_y = \sqrt{\frac{\sum(d_i^2)}{N-2}}$	(2) $s_m = \sqrt{\frac{s_y^2 \times N}{D}}$	(3) $s_b = \sqrt{\frac{s_y^2 \times \sum(x_i^2)}{D}}$	(4) $LOD = \frac{3s_{y(blank)}}{m}$
(5) $LOQ = \frac{10s_{y(blank)}}{m}$	(5) $F_{calc} = \frac{s_1^2}{s_2^2}$	(6) $T_{calc} = \frac{d_{bar}}{s_d} \sqrt{N}$	(7) $s_d = \sqrt{\frac{\sum(d_i - d_{bar})^2}{N-1}}$
(8) $D = \frac{\sum(x_i^2)}{\sum x_i} \sum x_i$ $N$			

## Results / Data Analysis / Discussion

In the FAAS portion of this experiment, calibration curves must be made in order to determine the concentrations of Samples A, B, and C. The FAAS instrument output provided three replicate measurements of absorbance for each sample from which a calibration curve can be made. The calibration curves contain only the average of the three absorption values for each concentration. The linear regression line of each calibration curve will be used to plug in the measured absorbance of Samples A, B and C and solve for the concentration. Figures 7 and 8 display the calibration curves for the Group Data and the Class Data, respectively. The smaller graph in the upper left is a zoomed in image of the low- concentration portion of the curve.

Sample	Group Data (ppm)	Class Data (ppm)
A	1.37	1.68
B	2.41	2.56
C	2.95	3.19
Duplicate A	1.33	1.68
LFM	0.38	1.14
LFB	2.32	1.50

**Table 1:** Sample Concentrations for Group and Class Data

The error bars are  $\pm 1$  standard deviation of the three measurements of each concentration. Table 1 displays the results of the experiment: the concentrations of lead in each unknown Sample found using the linear equations for each calibration curve, displayed in Figures 7 and 8. The concentration of the LFM given by the instrument had to be back-calculated to get the original concentration of the sample.

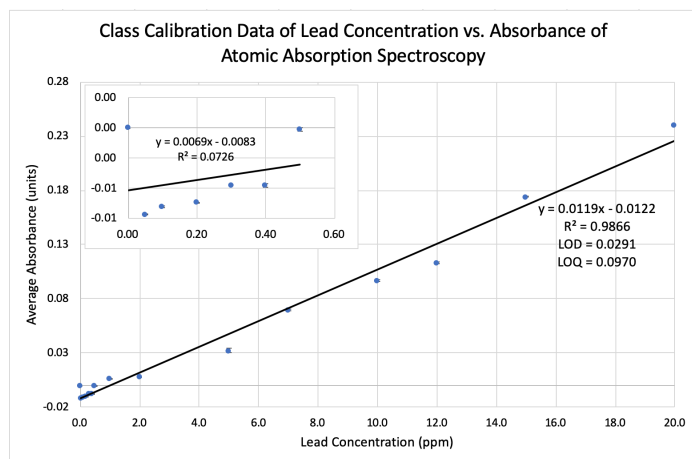


Figure 7: Group FAAS Calibration Curve

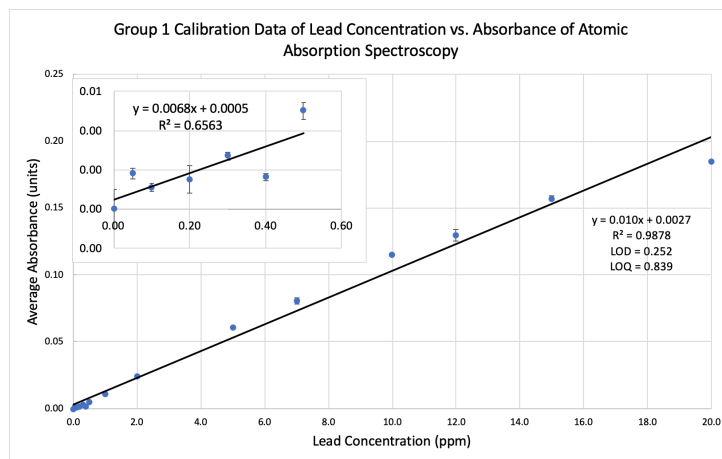


Figure 8: Class FAAS Calibration Curve

A statistical linear regression analysis of the calibration curves was done. The Group Data linear regression line has an  $R^2$  value of 0.9878, while the Class Data calibration curve has an  $R^2$  value of 0.9866. Because the Group Data  $R^2$  is closer to 1, the Group Data follows a more linear pattern. Additionally, the standard deviations of y, m (slope), and b (y-intercept) for each data set were found using Equations (1), (2), and (3), respectively. These standard deviation values can be found in Table 2, and the calculations can be found in Excel. Since the standard deviations of the Group Data are all lower than that of the Class Data, it is suggested that the Group Data has more error. This is the reason why the LOD and LOQ reported are calculated from the Class Data.

	Group Data	Class Data
<b>s(y)</b>	0.0075	0.0093
<b>s(m)</b>	0.00031	0.00038
<b>s(b)</b>	0.0025	0.0031

Table 2: Standard Deviations of y, m, and b

A statistical comparison was conducted to compare the accuracy and precision of the Group Data and the Class Data sets. First, a two-tailed t-Test was utilized with equations (7) and (8). The  $t_{\text{calc}}$  value was 1.12, which is less than the  $t_{\text{table}}$  value of 2.13, meaning that there is **no difference between the accuracies** of the data sets at the 95% confidence level. Next, an f-Test was done using equation (6). The  $f_{\text{calc}}$  value was 1.41, which is less than the  $f_{\text{table}}$  value of 2.95, meaning that there is **no difference between the precision** of the data sets at the 95% confidence level. The calculations for these statistical tests can be found in Excel.

An outside lab sent data from their Lead Ion Selective Potentiometer (Pb ISE) for a statistical comparison with the FAAS data to find out if there is a statistical bias in the precision and accuracies. The outside lab tested the lead concentrations in the same samples this lab tested, allowing for comparisons to be drawn. First, a one-tailed t-Test was done with equations (7) and (8). The  $t_{\text{calc}}$  value was 1.10, which is less than the  $t_{\text{table}}$  value of 1.94, meaning that there is **no difference between the accuracies** of the data sets at the 95% confidence level. Next, an f-Test was completed using equation (6). The  $f_{\text{calc}}$  value was 3.91, which is less than the  $f_{\text{table}}$  value of 4.28, meaning that there is **no difference between the precision** of the data sets at the 95% confidence level. The calculations for these statistical tests can be found in Excel. Therefore, there is no statistical bias between the two instruments. Therefore, either instrument can be used with the same confidence. Since FAAS is not portable, it should be chosen for use in a laboratory. However, if a sample needs to be quantified in the field, Pb ISE is more mobile and would be a viable option.



No G-Test was conducted for either set of data analysis. The purpose of a G-Test is to determine if a certain data point is an outlier so it can be removed. When making calibration curves, however, if there is a data point that resembles an outlier, the measurements are simply retaken. Therefore, there was no statistical need for a G-Test in this analysis.

The purpose of the FAAS experiment was to quantify the amount of lead in three samples of unknown concentrations. The resulting concentrations are listed in Table 1. All of the samples are much more concentrated than the EPA recommended maximum Pb concentration (15 ppb).<sup>4</sup> This is a health risk to anyone who drinks this water. If the concentration of a sample is below the instrument's LOQ, it cannot be quantified by the calibration curve produced by that instrument. The LOQ for the Shimadzu AA-7000 is 0.0970 ppm, therefore all of the samples were able to be quantified. Additionally, a sample isn't able to be detected by an instrument if its concentration is below the LOD, but that has not occurred in this experiment either.

The statistical comparison between the Group Data and the Class Data shows that they are not statistically different in accuracy or precision. This means that even though the samples were made on different days by different groups, the results were still the same. The statistical comparison between the FAAS method and the Pb ISE method also shows that they are not statistically different in accuracy or precision. This means that either method can be used to test samples and the results will not be statistically different. These statistics results are either due to the culmination of various errors, or to the true versatility of this experiment.

There are various possible sources of error in this experiment. Firstly, other groups may have incorrectly prepared their high/low concentration solutions which Group 1 used in their Group Data set. Since these concentrations are in the calibration curve, they could make the regression equation less accurate. Secondly, the solutions that had concentrations lower than the limit of detection of the instrument may have had incorrect concentrations reported. Since these concentrations are also in the calibration curve, they could also make the regression equation less accurate. This source of error is likely why the zoomed in graphs in Figures 7 and 8 are much less linear than the full-size graphs. All of the concentrations that low are below the limit of detection, leading to inaccurate readings. Thirdly, the nebulizer in the Shimadzu AA-7000 was broken during the week of Group Data collection, but it was fixed for the week of Class Data collection. This should have caused considerable error in the Group Data. Surprisingly, there was no difference between the precision or accuracy of the Group Data and the Class Data.

In the ICP-Q-MS portion of this experiment, calibration curves were created in order to determine the concentrations of lead and iron in the samples. The ICP-Q-MS instrument output provided three replicate measurements of relative intensity for each sample from which a calibration curve can be made. The calibration curves contain the average intensity of the blank subtracted from the average of the three intensity values for each concentration. This value will be referred to as the net intensity. The linear regression line of each calibration curve was used to plug in the measured net intensity of each sample and solve for the concentration. Four calibration curves were made in total. The calibration curves in Figures 9 and 10 display the TERL standard data of lead and iron, respectively. The calibration curves in Figures 11 and 12 display the Group standard data of lead and iron. The error bars are  $\pm 1$  standard deviation of the three measurements of each concentration. This value was back calculated from the RSD output from the instrument software. Because all of the standards had concentrations above the LOD and LOQ, all of the data points were kept on the calibration curves.

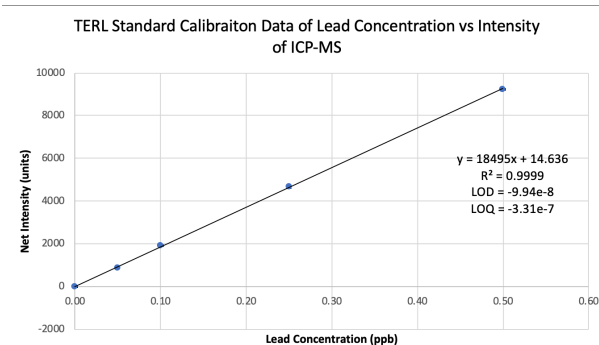


**Figure 9:** TERL Lead ICP-MS Calibration Curve (Background Subtracted)

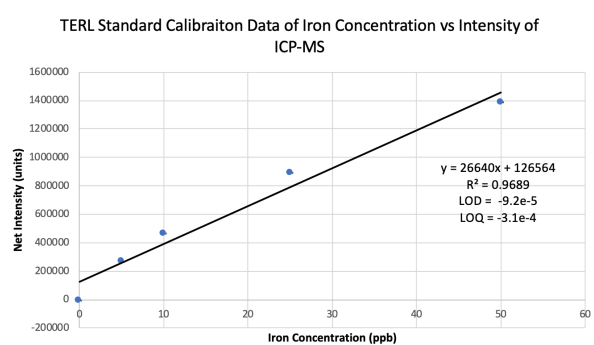


**Figure 10:** TERL Iron ICP-MS Calibration Curve (Background Subtracted)

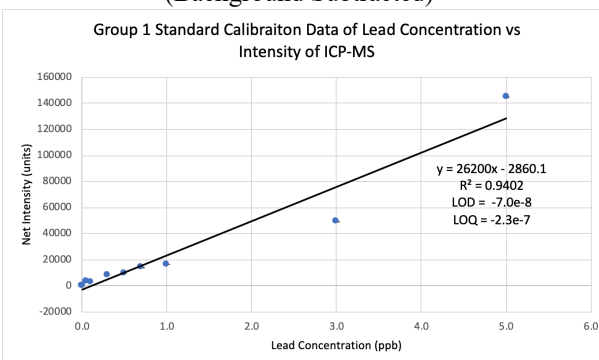


**Figure 11:** Group Lead ICP-MS Calibration Curve (Background Subtracted)

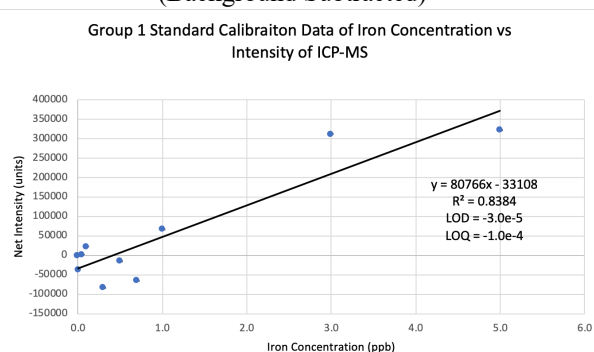


**Figure 12:** Group Iron ICP-MS Calibration Curve (Background Subtracted)

Table 3 displays the results of the experiment: the concentrations of lead and iron in each sample of drinking water from the Ohio State Campus. These concentrations were calculated using the linear equations for each calibration curve, displayed in Figures 9-12, to solve for the concentration of each sample and field blank. The field blank concentration subtracted from the sample concentration for each location yielded the final concentration values. The purpose of the field blank subtraction is to account for the metal ions that entered the samples through the air at the sample location. Instrumental drift was accounted for by multiplying each concentration by the percent change in measurement of the standard checks. See Excel for calculations. The final concentrations of a few samples were calculated to be negative, which is physically impossible. For those samples, the method blank had higher value than the sample concentration, resulting in a negative number during subtraction of the blank. This occurrence also resulted in negative standard deviations and LOD/LOQs. Because the Fe concentrations are more negative than the Pb concentrations, there was likely more Fe in the blank solution.

A statistical linear regression analysis of the calibration curves was done. The TERL Lead Data linear regression line has an  $R^2$  value of 0.999, while the Group Lead Data calibration curve has an  $R^2$  value of 0.9402. In addition, the TERL Iron Data linear regression line has an  $R^2$  value of 0.9689, while the Group Iron Data calibration curve has an  $R^2$  value of 0.8384. Because the data collected using the TERL standards had an  $R^2$  value that is closer to 1, that data follows a more linear pattern than the data collected using the Group standards. Furthermore, it can be said that the TERL standards were more accurate than the Group Standards. Therefore, all interpretation of the data will be done using only the TERL Standard data sets. Additionally, the standard deviation of  $y$  for each data set were found using equation (1). These standard deviation values were used to formulate the  $y$ -axis error bars in the calibration curves. Calculations can be

found in Excel. Almost all of the errors were calculated to be so small that the error bars are enveloped by the data point. The y-errors were likely small because they were calculated from the RSD, the percent standard deviation of the three replicate measurements, and the instrument is very precise, yielding nearly the same result in each replicate measurement. The TERL Lead Data linear regression line has an  $s_y$  value of 51.2, while the Group Lead Data calibration curve has an  $s_y$  value of 11559.7. In addition, the TERL Iron Data linear regression line has an  $s_y$  value of 111339.5, while the Group Iron Data calibration curve has an  $s_y$  value of 62029.8. These calculations were done using Equation (1). Overall, the lead  $s_y$  values were much lower than that of iron, meaning that the instrument was able to measure the lead intensities more accurately. This occurrence may be due to isotopic interferences.

Isotopic interferences are the most prominent type of interference in analysis using ICP-MS. It occurs when two analytes in the sample have isotopes of the same mass. Because the instrument detects different elements based on mass, it will classify the two different elements as one.<sup>15</sup> For example, Fe and Ni both have isotopes at mass 58, so any signal measured at 58 m/z will have contributions from both metals. This interference makes it difficult to determine the actual intensity of the desired element. Some methods of avoiding this issue are performing reactions with an inert gas such as He or NH<sub>3</sub> and using high-resolution mass spectrometry. For this experiment, the method used was to choose to measure the intensity of a particular isotope of each analyte has a unique mass in the sample solution. In this experiment, lead was analyzed. The isotopic distribution of lead was expected to be 1.4% <sup>204</sup>Pb, 24.1% <sup>206</sup>Pb, 22.1% <sup>207</sup>Pb, and 52.1% <sup>208</sup>Pb.<sup>16</sup> The data collected through ICP-MS does roughly support these expectations. For example, in Standard 9, the abundance of each isotope was 0.96% <sup>204</sup>Pb, 26.3% <sup>206</sup>Pb, 19.7% <sup>207</sup>Pb, and 53.1% <sup>208</sup>Pb. These values are only slightly different from the expected values. The monoisotopic mass of lead is  $(203.9730)(0.014) + (205.9745)(0.241) + (206.9759)(0.221) + (207.9767)(0.521) = 207.9$ . Because <sup>208</sup>Pb is the most abundant isotope of lead and no other substances in the sample had the same mass, it was chosen to be the measured isotope. For the same reasons, the <sup>56</sup>Fe isotope was chosen.

Sample	Concentration of Pb, TERL Standards (ppb)	Concentration of Fe, TERL Standards (ppb)	Concentration of Pb, Group Standards (ppb)	Concentration of Fe, Group Standards (ppb)
Barrett House	-0.00128	0.592	-0.000884	0.122
Busch House	0.00221	-1.82	0.00153	-0.376
RPAC	0.0190	-3.09	0.0131	-0.637
Campbell Hall	0.0965	-0.362	0.0667	-0.0745
Hopkins Hall	0.0986	-1.47	0.0681	-0.303
NIST	3.94	-2.40	2.83	1.62

**Table 3:** Average concentrations of Pb and Fe in drinking water found by ICP-Q-MS

Lead and iron concentrations in drinking water samples from five locations around the Ohio State Campus were quantified using ICP-Q-MS. The resulting concentrations are listed in Table 3. Barrett House, Busch House, RPAC, Campbell Hall, and Hopkins Hall had lead concentrations of -0.00128, 0.00221, 0.0190, 0.0965, 0.0986 ppb and iron concentrations of 0.592, -1.82, -3.09, -0.362, -1.47, and -2.40 ppb, respectively. The NIST standard contained 3.94 ppb Pb and -2.40 ppb Fe. The negative concentrations are caused by the blank having a higher

concentration than the sample. All of the samples are well below the EPA recommended maximum Pb concentration of 15 ppb and Fe concentration of 300 ppb.<sup>(EPA)</sup> Fortunately, this means that there is no health risk of lead or iron poisoning from drinking the OSU campus water at these locations. Some possible sources of the metals that were found in the samples are portions of lead piping and iron from human and animal waste or iron industry machinery that touches large quantities of water. Sources of error in this experiment may include contamination of the samples by keeping the containers open for too long which would artificially raise the concentrations and making inaccurate standards which forms an inaccurate calibration curve.

For the  $\mu$ PAD portion of this experiment, the  $\mu$ PADs themselves had to be developed. In order to do this, many tests had to be run in order to optimize the device parameters. During the first week of development, 3% sodium carboxymethylcellulose preconcentrate solution was developed.<sup>4</sup> First, Group 1 attempted to make the solution using 3.0408 g sodium carboxymethylcellulose, ~10 g zirconium silicate, and 100 mL nanopure water. The mixture was not homogeneous; it formed thick mucus-like liquid with some large chunks of undissolved powder. Group 1 then attempted dissolving the sodium carboxymethylcellulose in methanol instead of water in hopes of better solubility. Unfortunately, the solids appeared to have less solubility in methanol than water. Next, the mixture was attempted in nanopure water again, but this time the solids were added slowly with vigorous mixing. The solids appeared to dissolve better, and then mixture was left mixing with a magnetic stir bar over the following week. The resulting solution was white and a thick corn syrup viscosity mixture. Group 1 deemed this version acceptable. The initial method of applying the preconcentrate solution was supposed to consist of dipping the  $\mu$ PAD into the solution, but the solution was too viscous. The Group determined the new application procedure to be applying the preconcentrate with a medicine dropper, spreading it with a gloved finger, and then allowing it to dry.



**Figure 13:** Left: Plain paper  
Right: After melting wax

During the second week of development, wicking ability and indicator testing was conducted. Wicking ability testing was conducted in order to find the optimal time to apply the preconcentrate solution. The two possible times are before and after melting the wax. These two conditions were tested as well as a non-preconcentrated  $\mu$ PAD. The non-preconcentrated  $\mu$ PAD exhibited very quick wicking, as shown in Figure 13. The  $\mu$ PADs preconcentrated after melting displayed very slow wicking abilities (Figure 13) which are not ideal. The  $\mu$ PADs preconcentrated before having their wax melted had issues with the wax melting through the paper completely, so they could not be used. Therefore, the chosen

time to apply the preconcentrate was after melting the wax in order to ensure the complete melting of the wax.

Indicator testing was conducted to ensure that the 15 ppb indicator would react with the 0, 3, 6, 9, 12, and 15 ppb lead standards on both preconcentrated and not preconcentrated paper. No colors, neither yellow nor pink, were visible on any paper, as seen in Figure 14. Based on these results, it was concluded that the concentrations of both the

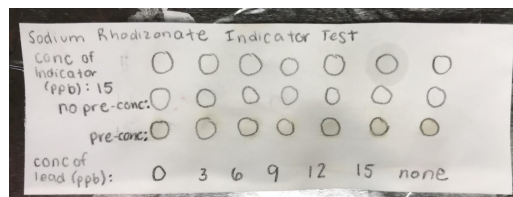


**Figure 14:** 15 ppb indicator tested with various concentrations of lead standards.



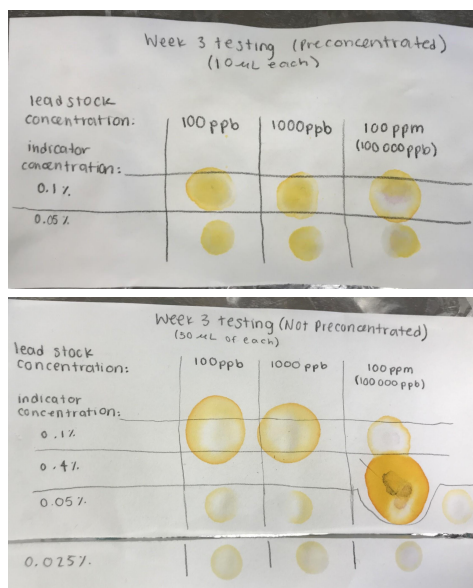


**Figure 15:** Top: Preconcentrated paper indicator tests  
Bottom: Non-preconcentrated paper indicator tests

The new experimental method implemented was the accumulation method. It involves placing multiple aliquots of the sample water on the testing area and letting it dry before adding indicator to accumulate a greater molar equivalent of lead. This technique increases the concentration of lead by a negligible amount. In order to test if this new method works, testing arrays were set up. Test squares were used instead of a full sheet of paper in order to stop the lead from wicking out into the surrounding paper, so it will stay concentrated in the testing area. The aliquot size was determined to be 10  $\mu\text{L}$  for this test in order to cover the surface area of the test squares. The concentrations of lead standards tested were 20, 40, 80, and 100 ppm. The number of aliquots tested were 6, 10, and 15. All of these variables were tested on both preconcentrated paper and non-preconcentrated paper and with 0.05% and 0.1% indicator, as seen in Figure 16. Upon looking at both arrays overall, the 0.1% indicator array is more orange, and the 0.05% indicator array is more pink. This signifies that the 0.1% indicator is too concentrated to allow for optimal pink detection. Therefore, 0.05% is the optimal indicator concentration, so all of the following observations are made just by looking at the 0.05% array. When

indicator and the lead standards were too low for detection by the human eye.

Based on the results of the previous week, the lead standard and indicator concentrations were increased for testing during Week 3. The new lead standards were 100 ppb, 1 ppm, and 100 ppm. The new indicator concentrations were 0.4%, 0.1%, 0.05%, and 0.025%. They were tested against each other on both preconcentrated and non-preconcentrated paper, as seen in Figure 15. Initially, the 0.4% and the 0.025% indicator concentrations were deemed unsuitable for the  $\mu\text{PAD}$ . The 0.025% was too light to be able to detect any pink color, while the 0.4% was too dark to be able to detect any pink color. The 0.1% and 0.05% indicator will continue on to further testing. There was no pink color to indicate the detection of lead except extremely faintly in the 100 ppm lead standard on the preconcentrated paper. Because this relatively high concentration of lead was barely detectable, a new technique needed to be implemented in order to achieve a lower LOD.

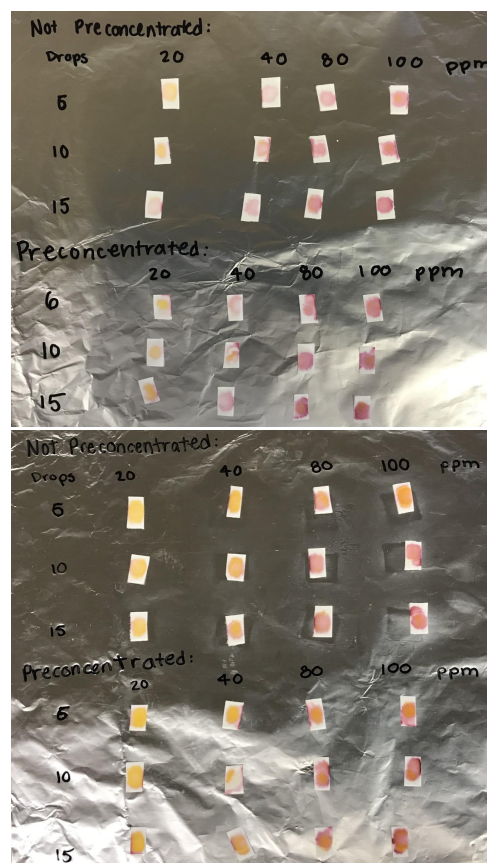


**Figure 16:** Top: 0.05% indicator test  
Bottom: 0.1% indicator test



comparing the preconcentrated and the non-preconcentrated paper, the preconcentrated paper was a more intense pink color and faded more slowly. Therefore, our final design will be preconcentrated. Finally, the lowest LOD needed to be determined. There was detectable pink in the 6 aliquots of 20 ppm lead standard, which was the lowest tested. Therefore, more tests were conducted to see if the LOD could be lowered further.

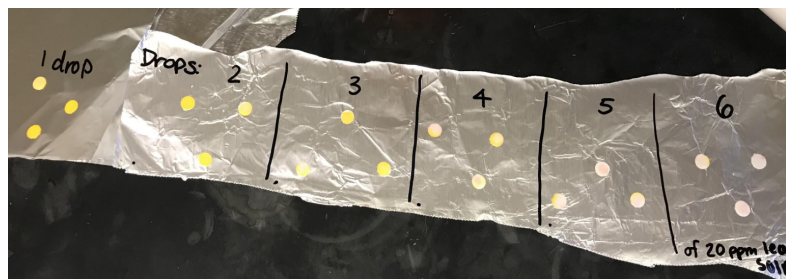


Figure 17: Aliquot testing

more representative of the  $\mu$ PAD design than test squares. The lowest detectable number of aliquots was 3, but not all three of the disks turned pink. 6 aliquots was the only amount that had pink detectable in all three disks, meaning that was fully reproducible. Therefore, the final  $\mu$ PAD design will require 6 aliquots of sample water.

Finally, the lowest detectable concentration of lead was attempted to be decreased. 10 ppm lead standard solution was tested against 20 ppm. 6 aliquots of each were placed on the  $\mu$ PAD, allowed to dry, and then 1 drop of 0.05% indicator was placed on each well. The 10 ppm well was not detectable, but the 20 ppm well was detectable. Displayed in Figure 18. Therefore, the LOD of the final  $\mu$ PAD design is 20 ppm lead using 6 aliquots of size 3  $\mu$ L and one aliquot of 0.05% sodium rhodizonate indicator on preconcentrated paper, as shown in Figure 19 and described in Methods.

One source of error in this experiment is contamination from the lab bench. If lead solution had been spilled on the lab bench and a  $\mu$ PAD had been run on top of the contaminated area without tape on the back, the indicator could have reacted with lead from the table. Another source of error is uncalibrated micropipettors. All of the lead standards were made using micropipettors and their last calibration date is unknown, meaning that the standards may be inaccurate. Additionally, using the same indicator for the entirety of one day may have introduced some error because the indicator degrades over time, rendering it less active.

In the future, Group 1 would like to continue the development of the  $\mu$ PAD. Some design features that may be introduced include multi-elemental analysis and a high concentration control well. The multi-elemental analysis feature would allow the user to test for at least one other heavy metal in their water, such as iron. The high concentration control would reduce the number of false negatives, because the user would be aware that the high concentration well is supposed to turn pink. Additionally, the preconcentrate shelf life should be tested because the  $\mu$ PADs are going to be sold already preconcentrated. Finally, Whatman 4 paper should be tested due to its large pores which may allow for better detection results.

First, the number of aliquots of sample water was attempted to be decreased. 1, 2, 3, 4, 5, and 6 aliquots were tested on test disks, as shown in Figure 17. The aliquot size was 3  $\mu$ L, which covers the surface area of one test disk. The disk design was used because it is



Figure 18: LOD testing; 10 and 20 ppm

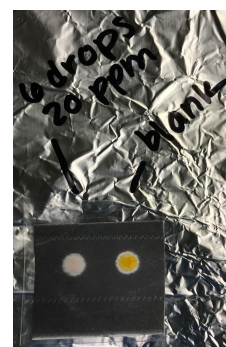


Figure 19: Final Design

## Conclusion

In the FAAS portion of this experiment, the concentrations of lead in various samples were able to be quantified, but the values lower than the instrument's limit of detection may not be accurate. It was statistically determined that the Group Data Set and the Class Data Set are not statistically different, and the methods of FAAS and Pb ISE are also not statistically different, so these methods can be used for the same types of experiments. FAAS is a reliable method of quantification of lead in water as long as the samples are within the LOD and LOQ. Using the class data set, the LOD and LOQ of the spectrophotometer were found to be 0.0291 and 0.0970, respectively. Therefore, the concentrations of lead in samples A, B, C, A Duplicate, LFM, and LFB were found to be 1.6, 2.56, 3.19, 1.68, 1.14, and 1.50 ppm, respectively. This study provides information about two methods of determining lead content in water. The ability to quantify lead in water is extremely important due to the detrimental effects of lead on the human body.<sup>1</sup>

In the ICP-Q-MS portion of this experiment, drinking water from various locations around the Ohio State Columbus Campus was analyzed for lead and iron content. ICP-QMS was used to quantify the heavy metal concentrations in the samples. Barrett House, Busch House, RPAC, Campbell Hall, and Hopkins Hall had lead concentrations of -0.00128, 0.00221, 0.0190, 0.0965, 0.0986 ppb and iron concentrations of 0.592, -1.82, -3.09, -0.362, -1.47, and -2.40 ppb, respectively. The limit of detection and limit of quantification of the ICP-QMS instrument were found to be  $-9.94\text{e-}8$  and  $-3.31\text{e-}7$ , respectively. The negative concentrations are caused by the blank having a higher concentration than the sample. All of the samples are well below the EPA recommended maximum Pb concentration of 15 ppb and Fe concentration of 300 ppb.<sup>4</sup> Fortunately, this means that there is no health risk of lead or iron poisoning from drinking the OSU campus water at these locations. This method could be used in future work for quantifying other heavy metals in drinking water samples.

In the  $\mu$ PAD portion of the experiment, a long series of parameter testing led to the development of a functional  $\mu$ PAD. It wields a dual-well system, one reaction well and one control well, and has a LOD of 20 ppm. The procedure of using the  $\mu$ PAD is very simple; the general public would likely not have trouble with it. Because the  $\mu$ PAD is so small and light, it is a very portable device. It would also be sold relatively cheaply due to its simple components. Because of its low price, ease of use, and portability, the  $\mu$ PAD seems to be the best method of detecting lead in the field or in-home. Once the LOD is lowered to at least 15 ppb, the legal maximum lead concentration,  $\mu$ PADs will have the opportunity to change societal standards for water.<sup>4</sup> All citizens may one day be able to test their water in their own home with  $\mu$ PADs.

## References

1. Gray, N.F., *Drinking Water Quality and Solutions.*; Cambridge University Press, 2008.
2. Clark, A., *The Poisoned City: Flint's Water and the American Urban Tragedy.*; Henry Holt and Company, 2018.
3. Rangan, C., *Diagnosis and Treatment of Pediatric Iron Ingestion.*; California Poison Control System, 2003.
4. United States Environmental Protection Agency Office of Ground Water and Drinking Water., *National Primary Drinking Water Regulations.*; National Service Center for Environmental Publications, 2016.
5. Hashimi, A.S., *A Guide To Spectroscopy for Used Oil Analysis.*; AZO Materials, 2016.
6. Karn, Nicole, *Carmen FAAS Page.*; Ohio State, 2019.
7. Walsh, A., *The Application of Atomic Absorption Spectra to Chemical Analysis.*; Pergamon Press Ltd., 1955.
8. Henderson, B., *Use of Ion-molecule Reactions in Inductively Coupled Plasma Mass Spectrometry (ICP-MS) to Improve Selenium Analysis Accuracy and Detection.*; OSU Honors Thesis
9. Nisi, S., *ICP-MS measurement of natural radioactivity at LNGS.*; World Scientific, 2017.
10. Harris D.C., *Quantitative Chemical Analysis.*; W.H. Freeman and Company, 2016.
11. Martinez, A. W.; Phillips, S. T.; Butte, M. J.; Whitesides, G. M. Patterned Paper as a Platform for Inexpensive, Low-Volume, Portable Bioassays. *Angewandte Chemie International Edition* 2007, 46 (8), 1318–1320.
12. Jiang, X.; Fan, Z. H. Fabrication and Operation of Paper-Based Analytical Devices. *Annual Review of Analytical Chemistry* 2016, 9 (1), 203–222.
13. Lisowski, P.; Zarzycki, P. Microfluidic Paper-Based Analytical Devices ( $\mu$ PADs) and Micro Total Analysis Systems ( $\mu$ TAS): Development, Applications and Future Trends. *US National Library of Medicine National Institutes of Health*. 2013.
14. Satarpai, T.; Shiowatana, J.; Siripinyanond, A. Paper-Based Analytical Device for Sampling, on-Site Preconcentration and Detection of Ppb Lead in Water. *Talanta* 2016, 154, 504–510.
15. Spectroscopy Editors, *Reducing the Effects of Interferences in Quadropole ICP-MS.*; Solutions for Materials Analysis, 2010.
16. Meija, J., *Understanding Isotopic Distributions in Mass Spectrometry.*; Journal of Chemical Education, 2006.